

# Standing Wave Considerations in the Link Model of 60 GHz Directional Surface Wave Arrays

Prabhat Baniya and Kathleen L. Melde

Department of Electrical and Computer Engineering

University of Arizona, Tucson, AZ, USA

Email: pbaniya@email.arizona.edu; melde@email.arizona.edu

**Abstract**—This paper proposes an improvement of the link model of 60 GHz directional surface wave antenna arrays. Since the transmit and receive arrays share the grounded substrate, the total coupling power is contained in both space and surface waves. The dominant  $TM_0$  mode of the grounded substrate contributes to the surface wave coupling. In addition, it is shown that the finite extent of the substrate creates a  $TM_0$  standing wave. This wave is responsible for oscillations in the power coupling between the arrays as a function of their separation.

## I. INTRODUCTION

Surface wave antenna arrays have been used to increase the link transmission in situations when it is desirable to have the transmit (TX) and receive (RX) antennas in the same plane [1]. The presence of a common ground plane and substrate causes significant surface wave coupling between the microstrip antennas [2]. The relative contribution of space wave (radiation) and surface wave to the total link power was studied in [2] for various antenna types. The surface waves are the  $TM^z$  and  $TE^z$  modes of the grounded dielectric substrate [3]. The lowest order (dominant) mode is the  $TM_0$  which has a zero cutoff frequency. The fields under the patch metal will always excite this mode even on thin substrates with low dielectric constant as illustrated in Fig. 1. In this paper, we will consider the effect of the  $TM_0$  standing wave in the link power analysis of 60 GHz directional surface wave antenna arrays. This will improve the link model in [2] so that it has better agreement with the full wave simulation result for the arrays considered here. We will also improve the curve fit and uniqueness of the link model by incorporating the free space gain obtained from the simulated radiation pattern.

## II. ANTENNA ON A GROUNDED DIELECTRIC SUBSTRATE

The antenna substrate used in this work is a Rogers RO4003C with height  $h = 0.2$  mm, and dielectric constant  $\epsilon_r = 3.55$ . For this substrate, as shown in Fig. 1, only the dominant  $TM^z$  mode i.e.,  $TM_0$  can be excited at 60 GHz while the higher order  $TM^z$  and  $TE^z$  modes are cutoff [3]. The characteristic equation of the grounded dielectric substrate  $\epsilon_r \alpha_{z0} = \beta_{zd} \tan(\beta_{zd} h)$  was solved along with the separation equations  $\beta_{zd}^2 = \beta_0^2 \epsilon_r - \beta_{TM0}^2$  and  $\alpha_{z0}^2 = \beta_{TM0}^2 - \beta_0^2$  to find the air attenuation coefficient  $\alpha_{z0} = 0.19\beta_0$ , dielectric wave number  $\beta_{zd} = 1.59\beta_0$ , and propagation constant  $\beta_{TM0} = 1.02\beta_0$  of the  $TM_0$  mode where  $\beta_0 = 2\pi/\lambda_0$  and  $\lambda_0 = 5$  mm.

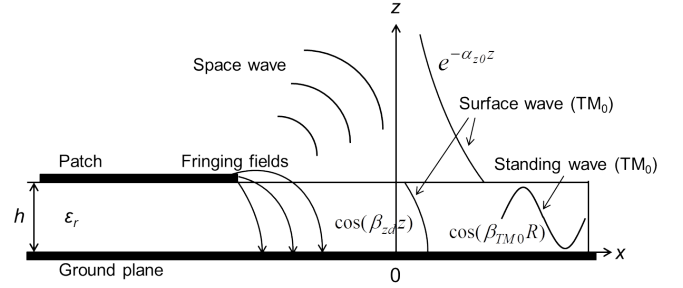


Fig. 1. Field distribution of the  $TM_0$  mode in a grounded dielectric substrate along with radiation from a microstrip antenna.

The  $z$ -component of the electric field of the  $TM_0$  surface wave in the air and dielectric respectively are as follows [3].

$$E_z^0 = -j(\beta_{TM0}^2 / (\omega\mu_0\epsilon_0)) A^d \cos(\beta_{zd}h) e^{-\alpha_{z0}(z-h)} e^{-j\beta_{TM0}x} \quad (1)$$

$$E_z^d = -j(\beta_{TM0}^2 / (\omega\mu_0\epsilon_0\epsilon_r)) A^d \cos(\beta_{zd}z) e^{-j\beta_{TM0}x} \quad (2)$$

At the air-dielectric interface  $z = h$ , there is a discontinuity in the  $z$ -component of the electric field i.e.,  $E_z^0 = \epsilon_r E_z^d$  (since the normal electric flux density has to be continuous), as shown in Fig. 1. The  $TM_0$  mode when it reaches the substrate edge is reflected back creating a standing wave pattern in the substrate. In air, this mode is diffracted at the edges. In addition to the  $TM_0$  surface wave, there also exists the space wave in air due to fringing fields from the patch metal to the ground plane.

## III. LINK MODEL WITH STANDING WAVES

An improvement of the transmission link equation in [2] with space, surface and standing wave coupling taken into account between two identically oriented antennas in the far-field of one another is as follows.

$$|S_{21}|^2 = G_3^2 \left( \frac{\lambda_0}{4\pi R} \right)^2 + G_2^2 \frac{\lambda_0}{4\pi^2 R} + 2G_3 G_2 \frac{\lambda_0}{4\pi R} \sqrt{\frac{\lambda_0}{4\pi^2 R}} + A_{TM0} \cos^2[\beta_{TM0}(R - R_0)] \quad (3)$$

where  $|S_{21}|$  represents the magnitude of the transmission coefficient between the TX and RX,  $R$  is their separation distance,  $G_3$  and  $G_2$  are the line-of-sight (LoS) free space (3D) gain and surface wave (2D) gain of the antennas respectively, and  $A_{TM0}$  is the normalized peak power (at separation  $R_0$ ) of the  $TM_0$  standing wave. The parameters  $G_2$  and  $A_{TM0}$  are

determined by curve fitting (3) with the  $|S_{21}|$  simulation data at different spacing  $R$  whereas  $G_3$  is simply taken from the simulated radiation pattern of the array. This will improve the uniqueness of the curve fitting solution as there is one less parameter to curve fit. The  $|S_{21}|$  full wave data is obtained by varying  $R$  from 10 mm to 20 mm in 0.2 mm steps. Note that the powers in the first three terms in (3) are in the form of traveling waves. Some portion of the power of the  $TM_0$  mode is in the form of standing wave that exists between the TX and RX because of the finite extent of the substrate. This was taken into account in (3) with an addition of the cosine squared term. This term causes oscillations in the power coupling as the separation between the TX and RX is varied.

#### IV. ANTENNA ARRAYS WITH LINK MODEL

The antenna considered is a two-element center fed circular patch array with four shorting vias under each patch, which is labeled in Fig. 2 as TX and RX along with the dimensions. The vertical gain component ( $G_0$ ) of the array in the  $xy$ -plane at 60 GHz is shown in the inset. The antenna has a low reflection coefficient ( $|S_{11}| < -17$  dB) at 60 GHz. The feed network is a  $T$ -junction power divider [1]. The electric field of the dominant  $TM_{01}$  mode of the antenna [4] can easily couple to the  $TM_0$  mode of the substrate and thus excite the surface waves. The  $TM_{01}$  mode of the center-fed circular patch can be expressed as follows.

$$E_z^{ant} = BH_0^{(2)}(\beta_{TM_0}R) \xrightarrow{R \rightarrow far} B \sqrt{\frac{2j}{\pi\beta_{TM_0}R}} e^{-j\beta_{TM_0}R} \quad (4)$$

where  $B$  is a constant that depends on the antenna geometry. The outgoing Hankel function in (4) in the far-field takes a form similar to (2) and represents the 2D spreading of the wave which is guided by the substrate as surface waves.

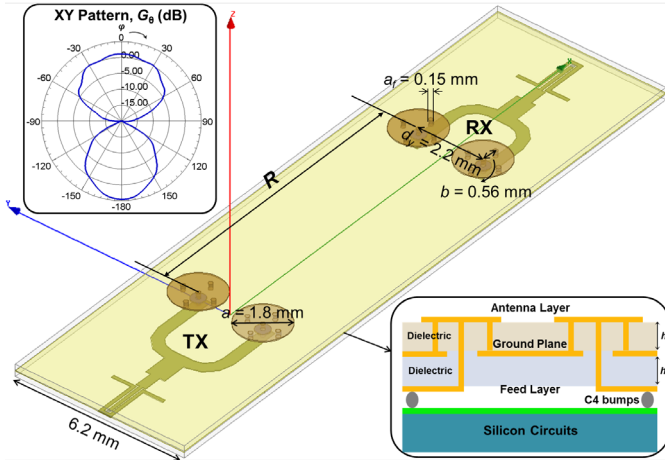


Fig. 2. A pair of two-element center fed circular patch arrays separated by distance  $R$ . In the inset, the 60 GHz  $G_0$  pattern (dB) in the  $xy$ -plane and layer stackup are shown.

The electric field distribution of the different waves in the plane parallel to the  $yz$ -plane midway between the TX and RX is shown in Fig. 3(a). The surface wave in air exists primarily near the interface. As shown in Fig. 3(b), the wave attenuates exponentially in air away from the interface while it varies as  $\cos(\beta_{zd}z)$  in the dielectric. Also, there is a discontinuity of the

electric field  $|E_z|$  at the interface as predicted in Section II. The normalized simulated and theoretical  $|E_z|$  curves agree well with slight deviation for  $z > 2$  mm. This can be attributed to the presence of the radiation field at and above the interface. The exponential decay applies only to the surface wave and the behavior of space wave away from the interface must also be considered.

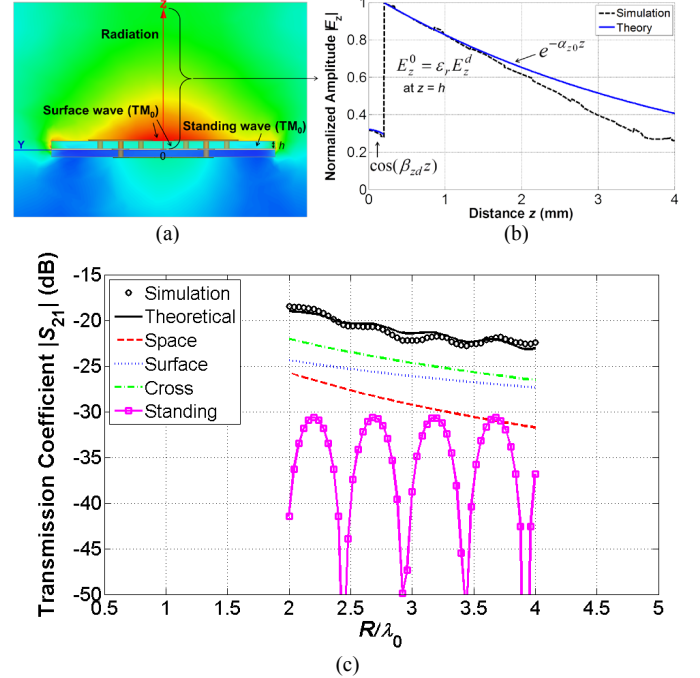


Fig. 3. (a) Electric field distribution at 60 GHz in the midway  $yz$ -plane. (b)  $|E_z|$  at 60 GHz along the  $z$ -axis in both the air and dielectric regions. (c) Decomposition of total link power into space, surface and standing waves.

The least squares method was used to curve fit (3) which resulted in  $G_2 = 0.54$  and  $A_{TM_0} = 0.001$ . The coefficient  $G_3 = 1.3$  was taken from the radiation pattern in the inset of Fig. 2 at  $\phi = 0^\circ$  (i.e., LoS direction) and used with  $R_0 = 11$  mm in (3). The relative contribution of the different waves to the total link power in (3) as a function of  $R$  is shown in Fig. 3(c). The  $TM_0$  standing wave in the substrate is responsible for fluctuations in the power coupling between the TX and RX.

#### ACKNOWLEDGMENT

This work was supported in part by the US National Science Foundation under Grant ECCS-1708458.

#### REFERENCES

- [1] P. Baniya, A. Bisognin, K. L. Melde, and C. Luxey, "Impact of gain and polarization in the design of reconfigurable chip-to-chip antennas," in *Proc. 10th Eur. Conf. Antennas Propag. (EuCAP)*, Davos, Switzerland, 2016, pp. 1–4.
- [2] C. Wang, E. Li, and D. Sievenpiper, "Surface-wave coupling and antenna properties in two dimensions," *IEEE Trans. Antennas Propag.*, vol. 65, no. 10, pp. 5052–5060, Oct. 2017.
- [3] C. A. Balanis, *Advanced Engineering Electromagnetics*, 2nd ed. Hoboken, NJ, USA: Wiley, 2012.
- [4] V. Gonzalez-Posadas *et al.*, "Approximate analysis of short circuited ring patch antenna working at  $TM_{01}$  mode," *IEEE Trans. Antennas Propag.*, vol. 54, no. 6, pp. 1875–1879, Jun. 2006.